EARTHQUAKE ENGINEERING AND STRUCTURAL DYNAMICS, VOL. 26, 759–777 (1997)

SEISMIC TESTING OF A BUILDING STRUCTURE WITH A SEMI-ACTIVE FLUID DAMPER CONTROL SYSTEM

MICHAEL D. SYMANS[1]* AND MICHAEL C. CONSTANTINOU[2]

[1] *Department of Civil & Environmental Engineering, Washington State University, Pullman, WA 99164, U.S.A.*
[2] *Department of Civil Engineering, State University of New York at Buffalo, Buffalo, NY 14260, U.S.A.*

SUMMARY

This paper describes shaking table tests of a multi-storey scale-model building structure subjected to seismic excitation and controlled by a semi-active fluid damper control system. The semi-active dampers were installed in the lateral bracing of the structure and the mechanical properties of the dampers were modified according to control algorithms which utilized the measured response of the structure. A simplified time-delay compensation method was developed to account for delays within the control system. The results of the shaking table tests are presented and interpreted and analytical predictions are shown to compare reasonably well with the experimental results. © 1997 by John Wiley & Sons, Ltd.

Earthquake Engng. Struct. Dyn., **26**, 759–777 (1997)

No. of Figures: 10. No. of Tables: 2. No. of References: 28.

KEY WORDS: fluid damper; damping; energy dissipation; structural control; semi-active control; scale-model testing

1. INTRODUCTION

A compromise between passive and active seismic response control systems has been developed recently in the form of semi-active control systems. Semi-active control systems maintain the reliability of passive control systems while taking advantage of the adjustability of an active control system. The three classes of control systems may be defined as follows. *Passive control systems* do not require an external power source for operation and utilize the motion of the structure to develop the control forces. Control forces are developed as a function of the response of the structure at the location of the passive control system. *Active control systems* require a large power source for operation of electrohydraulic actuators which supply control forces to the structure. Control forces are developed based on feedback from sensors that measure the excitation and/or the response of the structure. The feedback from the structural response may be measured at locations remote from the location of the active control system. *Semi-active control systems* typically require a small external power source for operation and utilize the motion of the structure to develop the control forces. Control forces are developed based on feedback from sensors that measure the excitation and/or the response of the structure. The feedback from the structural response may be measured at locations remote from the location of the semi-active control system.

Semi-active control systems have only very recently been considered for applications to large civil structures. As such, a major portion of the research in this area has been devoted to analytical and numerical studies in which a number of idealized assumptions are made. For example, both time delays in operation of

* Correspondence to: Michael D. Symans, Department of Civil and Environmental Engineering, Washington State University, Pullman, WA 99164-2910, U.S.A.

Contract grant sponsor: National Center for Earthquake Engineering Research; Contract grant numbers: 93-5120, 94-5103A.
Contract grant sponsor: Taylor Devices, Inc.
Contract grant sponsor: Moog, lnc.

CCC 0098–8847/97/070759–19$17·50

Received 29 July 1996
Revised 6 January 1997

the control system and the complexities of structural systems are often neglected (for example, see References 1–7). The validity of such assumptions must be evaluated through experimental research. Recent experimental studies on semi-active control systems have been performed by, for example, Feng and Shinozuka[8] (semi-active sliding friction bearings), Kobori *et al.*[9] (semi-active stiffness control device), Gavin *et al.*[10] and Makris *et al.*[11] (semi-active electrorheological damper), Kawashima *et al.*[12] and Patten *et al.*[13] (semi-active fluid damper), and Spencer *et al.*[14] (semi-active magnetorheological damper). A summary of the operation and behaviour of some of the above-mentioned experimentally tested semi-active control systems is given by Symans and Constantinou.[15] To the author's knowledge, there are currently (January 1997) no full-scale applications of semi-active control systems for seismic protection. However, it is also apparent that such applications may be realized prior to the end of this century.

With respect to the research described herein on semi-active fluid damper control systems, the work of Kawashima *et al.*[12] and Patten *et al.*[13] is most directly related. The device tested by Kawashima *et al.*[12] consisted of a fluid damper combined with an external bypass loop containing a servovalve. The behaviour of the device is controlled by varying the amount of fluid passing through the bypass loop. The device behaves essentially as an adjustable force device with hysteretic-type damping. The semi-active fluid damper tested by Patten *et al.*[13] also consisted of a fluid damper combined with an external bypass loop containing a control valve. The intrinsic behaviour of the tested damper is nonlinear. However, the device is made to behave as a linear viscous damper through appropriate adjustment of the control valve.

2. DESCRIPTION OF TESTED SEMI-ACTIVE DAMPERS

The semi-active fluid dampers described in this paper are based on the design of a passive fluid damping device which has been studied for applications in seismic energy dissipation[16,17] and seismic isolation[18] (see Figure 1). The passive portion of the semi-active fluid damper consists of a stainless steel piston rod, a bronze piston head, a piston rod make-up accumulator and is filled with a thin silicone oil. The piston head orifices are designed such that the fluid flow is altered according to the fluid speed resulting in a force output which is proportional to the relative velocity of the piston head with respect to the damper housing. The damper

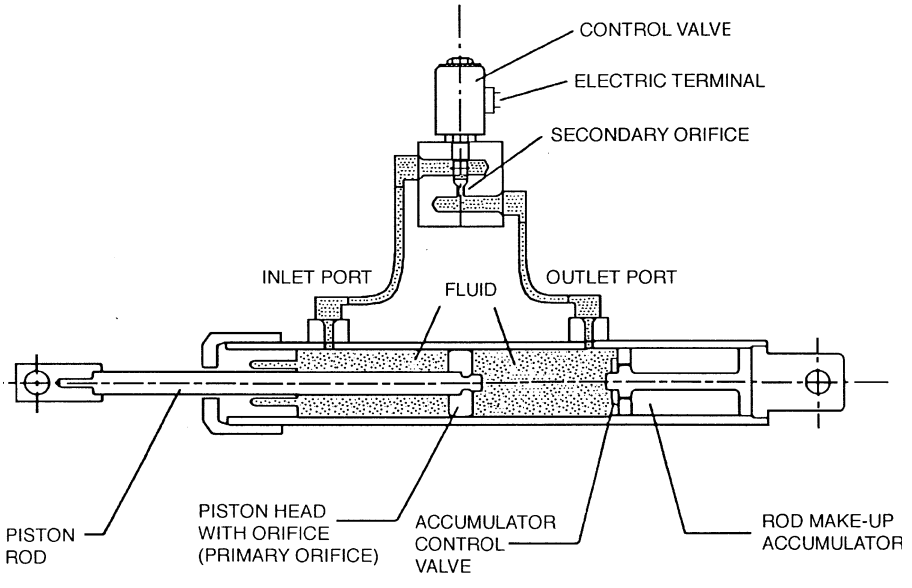

Figure 1. Construction of tested semi-active fluid damper

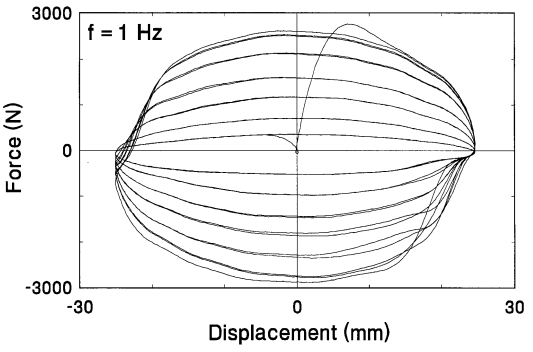

Figure 2. Response of semi-active damper when subjected to sinusoidal motion and with damping incrementally modified from high to low

weighed 61·6 N, had a fully compressed length of 192 mm, a housing diameter of 63·5 mm, and a maximum output force of 8900 N.

The passive fluid damper was modified to create a semi-active damper by including an external bypass loop containing a control valve (see Figure 1). The control valve is a normally closed direct-drive servovalve which was originally developed for control of the primary flight control servo-actuation system on the U.S. Air Force B-2 Stealth Bomber. The valve was designed to replace the conventional hydraulic amplifier pilot stage with a drive motor acting directly on the valve spool, eliminating the need for a source of hydraulic pressure to operate the pilot stage. The direct-drive servovalve offers fail-safe characteristics in that the loss of power causes the valve to become fully closed which in turn causes the semi-active damper to behave as a passive device with high damping characteristics. Furthermore, the servovalve requires a peak power of 3·5 W and can therefore operate on the power of batteries which is critical during an earthquake when the primary power source of a structure may fail.

The tested semi-active dampers behave essentially as linear viscous dampers with an adjustable damping coefficient and are capable of delivering a wide range of damping levels between an upper (valve closed) and lower (valve fully open) bound. This behaviour is demonstrated in Figure 2 which shows the damper response when subjected to sinusoidal motion at a frequency of 1 Hz and an amplitude of 25 mm and with the control valve initially closed and then incrementally opened throughout the test. The elliptical shape of the force–displacement loops is a clear indication of linear viscous behaviour. It is important to realize that the semi-active damper behaves as an adjustable parameter device rather than an adjustable force device. The interested reader is referred to Reference 15 for a detailed description of the testing and modelling of the semi-active fluid damper system.

3. DESCRIPTION OF TEST SET-UP FOR SEISMIC SIMULATIONS

A three-storey model structure was used for seismic simulation testing. The structure was a 1:4 scale steel moment-resisting frame which modelled a shear building by the method of artificial mass simulation.[19] The model did not represent a similitude-scaled replica of a full-scale building. Rather, the test structure was designed as a small structural system. The structure was bolted to the shaking table such that the main frames of the model were parallel to the motion of the table. The two frames of the structure which were perpendicular to the direction of motion were rigidly braced for all tests and ensured that there was no motion of the structure perpendicular to the direction of table motion. This resulted in the reduction of a three-dimensional structural system to, essentially, a planar frame. The mass of the three-storey structure was 2868 kg, each floor having an equal mass of 956 kg. The structure was tested with no dampers (bare frame) and with two semi-active dampers placed within the diagonal bracing of the first storey (see Figure 3).

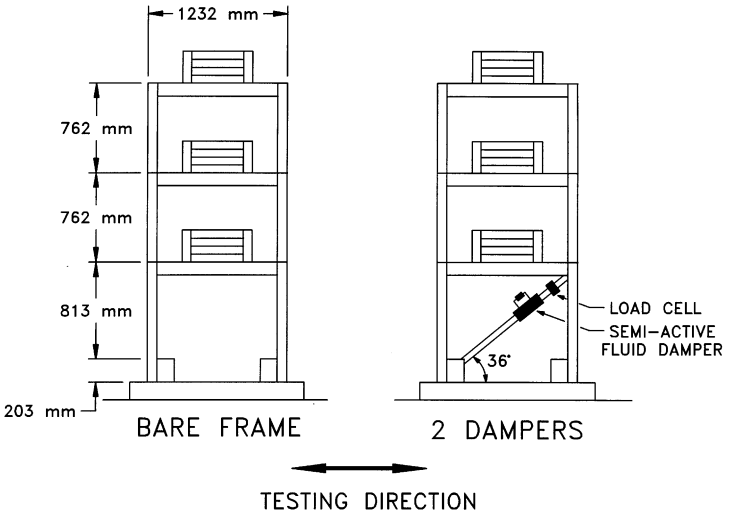

Figure 3. Shaking table test configurations for scale-model structure

Table I. Summary of experimentally identified properties of three-storey structure

		Bare frame			Semi-active dampers: low damping			Semi-active dampers: high damping		
Mode		1	2	3	1	2	3	1	2	3
Frequency (Hz)		1·80	5·80	11·40	1·80	5·84	11·43	1·85	6·04	11·48
Damping ratio (%)		1·74	0·76	0·34	4·13	3·90	1·07	14·41	18·79	4·83
Mode shapes	Floor 3	1·00	1·00	1·00						
	Floor 2	0·83	− 0·43	− 2·12						
	Floor 1	0·51	− 1·28	1·49						

The characteristics of the structure were identified using banded white noise (0–20 Hz) as input to the shaking table. The identification procedure is described in detail by Symans and Constantinou.[15] A summary of the identified properties of the model structure with and without semi-active dampers is provided in Table I.

Four different motions were used as input to the shaking table. Two of the motions were historical earthquake records (1940 El Centro earthquake (component S00E) and 1968 Hachinohe earthquake (component NS)). The historical earthquake records were compressed in time by a factor of two to satisfy the similitude requirements of the quarter-length scale model. The two other motions were a high-frequency version of the historical Hachinohe earthquake record and a harmonic signal of constant frequency and amplitude. In order to excite the test structure with earthquake motions of different intensity, the amplitude of the earthquake records was scaled for many of the shaking table tests.

A number of sensors were utilized to measure the response of the structure (absolute acceleration and displacement at each floor level) and the motion of the table (acceleration and displacement). A displacement transducer located along the axis of each damper measured the displacement of the piston rod with respect to the damper housing. Velocity measurements were obtained by passing displacement signals through analogue differentiators.

A block diagram showing the closed-loop shaking table tests with the semi-active dampers is provided in Figure 4. Both a data acquisition computer and a control computer were used during the tests. The control

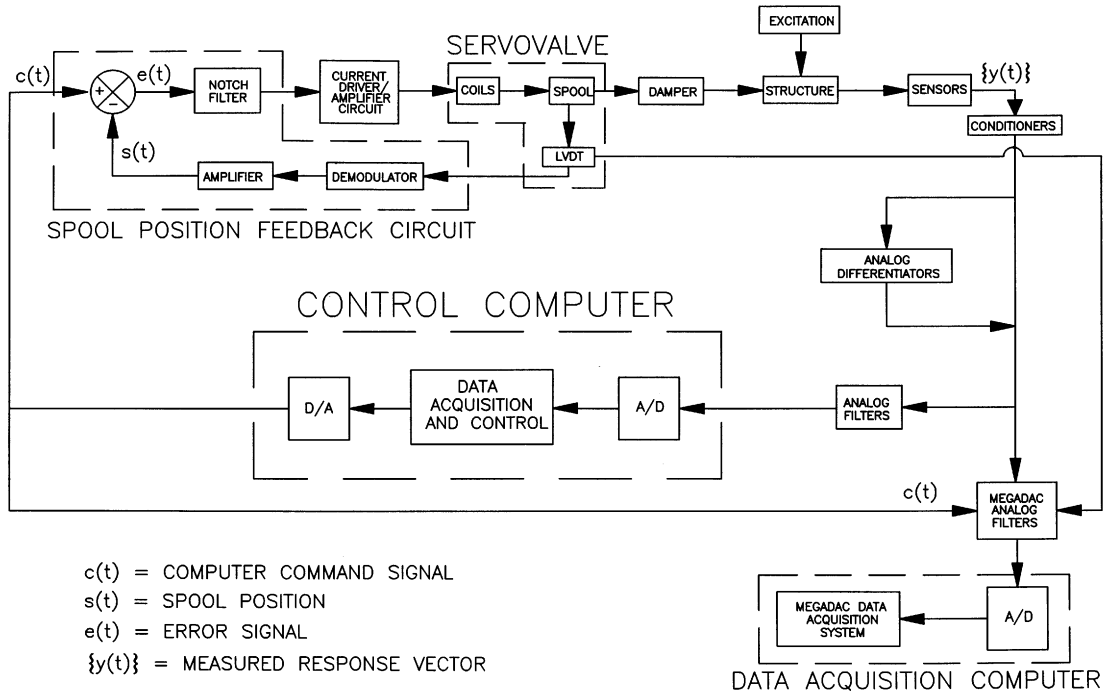

Figure 4. Block diagram of closed-loop shaking table tests with semi-active dampers

computer received signals from the measure response of the structure, processed the signals according to a pre-determined control algorithm, and sent an appropriate command signal to the semi-active damper valves. The response measurements were passed through six-pole low-pass Butterworth filters (cut-off frequency = 25 Hz) prior to entering the control computer. The control algorithms utilized for operation of the semi-active dampers were implemented on a PC computer with an INTEL™ 80386/25 MHz processor with two 12 bit data acquisition boards. Computer programs were written in the Microsoft QuickBASIC computer language (extended version 7.1) for implementation of the control algorithms. The sampling rate for control of the dampers was dependent on the control algorithm and ranged from about 160 pt/sec to about 530 pt/sec.

4. CONTROL ALGORITHMS FOR SEISMIC SIMULATION TESTING

As described in Section 2, the tested semi-active fluid dampers behave essentially as linear viscous dampers with an adjustable damping coefficient as given by the following expression

$$P(t) = C_{SA}\,\dot{u}(t); \quad C_{min} \leqslant C_{SA} \leqslant C_{max} \tag{1}$$

where $P(t)$ is the force in the damper, $\dot{u}(t)$ is the relative velocity of the damper piston head with respect to the damper housing, C_{SA} is the adjustable damping coefficient, and C_{min} and C_{max} are the lower and upper bound, respectively, on the adjustable damping coefficient. Control algorithms in which the constraint on the damping coefficient was not directly taken into account were developed. Rather, during experimental application of the control algorithms, the damping coefficient was clipped at the upper and lower bounds. In general, the control algorithms for the dampers may require that the dampers perform work on the structure such that the energy within the structural system is increased. The effect of clipping the damping coefficient at

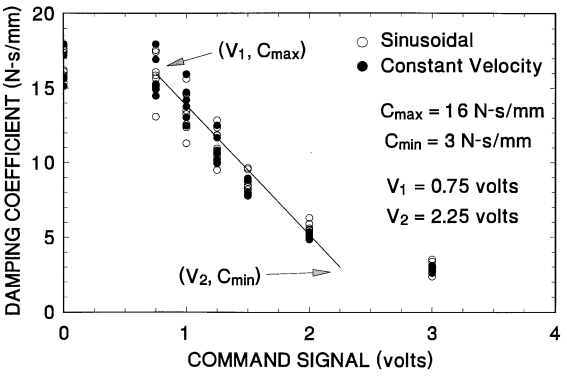

Figure 5. Relationship between experimental values of damping coefficient and command signal for semi-active dampers

the lower bound is to account for the inability of the semi-active dampers to perform this type of work on the structure (i.e. the dampers are only capable of absorbing energy). The issue of stability was not explicitly considered in the development of the control algorithms since the semi-active fluid dampers can only absorb energy; they are not capable of storing energy and thus inducing instability.

The relationship between the semi-active damper command signal and the damping coefficient is shown in Figure 5 for both sinusoidal and constant velocity cyclic testing over a range of frequencies from 0·25 to 4 Hz. The scatter in the data is primarily related to the frequency of testing. For semi-active damper command voltage levels between 0·75 and 2·25 V, the damping coefficient can be estimated by fitting a linear curve through the experimental data. In the control algorithms described in the following sections, the objective is to determine the damping coefficient which satisfies a given control objective and, based on the linear approximation shown in Figure 5, the appropriate command voltage is determined. The three storey structure was tested with two different control algorithms, one based on optimal control theory and the other based on sliding mode control theory.

4.1. Optimal control algorithm

The Linear Quadratic Regulator (LQR) optimal control algorithm has been investigated by a number of researchers for application to semi-actively controlled structures (e.g. see References 1, 2, 4, 13, and 20) and to actively controlled structures (e.g. see References 21 and 22). The general optimal control problem may be stated as follows: given a system subjected to external inputs, find the control which minimizes a certain measure of the performance of the system. The performance index for the LQR problem is given by the following scalar quantity:

$$J = \int_0^{t_f} (\{Z\}^T [Q] \{Z\} + \{d\}^T [R] \{d\}) \, dt \tag{2}$$

where t_f is the final time of the control interval, $\{Z\}$ is the state vector, $\{d\}$ is the control force vector, $[Q]$ is a positive semi-definite state weighting matrix, and $[R]$ is a positive-definite control force weighting matrix. The relative values assigned to the state and control weighting matrices reflect the importance attached to minimization of the state variables and control forces, respectively. The optimal control problem involves the minimization of the scalar functional J subject to the constraint equation given by the equation of motion of the system. The minimization process leads to the following control force vector:

$$\{d\} = -\tfrac{1}{2}[R]^{-1}[B]^T[P]\{Z\} = [G]\{Z\} \tag{3}$$

where $[G]$ is a constant control gain matrix, $[B]$ is the control force location matrix, and $[P]$ is the so-called Ricatti matrix which is obtained from the solution of the algebraic matrix Ricatti equation.[22] Note that to arrive at the control force vector described by equation (3), the earthquake input must be neglected. Further, it is important to realize that in both experimental and analytical studies, the values assigned to the weighting matrices are typically obtained through parametric studies that include the seismic excitation.

The three-storey model structure was tested with semi-active dampers in the first storey only. In this case, the control force vector of equation (3) becomes a scalar quantity given by

$$d = \sum_{n=1}^{3} (g_{1,n} u_n) + \sum_{n=1}^{3} (g_{1,n+3} \dot{u}_n) \tag{4}$$

where $g_{i,j}$ is the component of matrix $[G]$ in the ith row and the jth column and u_n and $\dot{u}_n$ are the relative displacement and relative velocity, respectively, of the nth floor. To facilitate comparison of results with previous work, the state and control force weighting matrices were selected to be identical to those used by previous researchers[21,22] in the study of an active tendon system on the same three-storey model structure. The algebraic matrix Ricatti equation was solved to obtain the Ricatti matrix, $[P]$, which was then substituted into equation (3) to obtain the 1×6 control gain matrix ($g(1,1) = 2316{\cdot}2$ N/cm, $g(1,2) = -1638{\cdot}4$ N/cm, $g(1,3) = 471{\cdot}1$ N/cm, $g(1,4) = 205{\cdot}8$ N s/cm, $g(1,5) = 23{\cdot}2$ N s/cm, $g(1,6) = 60{\cdot}3$ N s/cm). Assuming that the semi-active dampers behave according to a linear viscous dashpot model, accounting for the angle of inclination of the dampers, and recognizing the constraint on the damping coefficient given by equation (1), the necessary variation in the damping coefficient of each semi-active damper is given by

$$C_{SA} = \begin{cases} C_{\min} & \text{if } C^* \leqslant C_{\min} \\ (\eta \cos^2 \theta \dot{u}_1)^{-1} \left[\sum_{n=1}^{3} (g_{1,n} u_n) + \sum_{n=1}^{3} (g_{1,n+3} \dot{u}_n) \right], & \text{if } C_{\min} \leqslant C^* \leqslant C_{\max} \\ C_{\max} & \text{if } C^* \geqslant C_{\max} \end{cases} \tag{5}$$

where

$$C^* = \frac{1}{\eta \cos^2 \theta \dot{u}_1} \left[\sum_{n=1}^{3} (g_{1,n} u_n) + \sum_{n=1}^{3} (g_{1,n+3} \dot{u}_n) \right] \tag{6}$$

and η is the number of dampers and θ is the angle of inclination of the dampers. Note that equation (5) is considered to be a suboptimal damping coefficient since the damping coefficient constraint equation (equation (1)) was not considered in the optimization process.

4.2. Sliding mode control

The objective of the control algorithm described in this section is to track a specified trajectory, and in particular, for the case of stabilization the desired trajectory is identically zero. The combined error in velocity and displacement is used to determine the accuracy of tracking. Moreover, the algorithm can accommodate uncertainties that may exist in the parameters that define the structural system (e.g. mass, stiffness, and damping properties). The control algorithm is developed based on sliding mode control theory. A major advantage of sliding mode control theory is that the control of the structural system can be designed to be robust with respect to unmodelled dynamics, uncertain parameters, and external inputs. Sliding mode control theory begins with the design of a switching surface so that the response of the structural system has certain prescribed characteristics on the surface (e.g. the design is such that the system is asymptotically stable on the surface). Following the design of the switching surface, a control strategy is

developed which directs the response of the structural system onto the switching surface and attempts to maintain it there.

The sliding mode control algorithm utilized herein has been described by Ghanem and Bujakov[23] for applications to the control of Single-Degree-of-Freedom (SDOF) systems with uncertain parameters. The approach for SDOF systems was modified to adapt the algorithm for control of the three-storey model structure. Specifically, the three-storey structure was modelled as an equivalent SDOF structure which has the same natural frequency as the fundamental mode of the three-storey structure and the same base shear and overturning moment. A detailed description of the sliding mode control algorithm as used in this study is provided by Symans and Constantinou.[15]

5. SYSTEM TIME DELAYS AND METHODS OF COMPENSATION

There is a considerable amount of analytical research performed in the area of active and semi-active structural control in which the measurement of the response of the structure, the control computation, and the application of the control force are assumed to occur instantaneously. However, as a number of experimental studies have shown, time delays exist in the control system and, in general, must be considered to ensure stability of the structural system. Many methods of time delay compensation have been developed and experimentally tested (e.g. see References 22, 24, and 25).

Time delays may be conveniently separated into two components. In the following, it is assumed that the application of structural control is based on feedback that includes the response quantity $R(t)$ (e.g. displacement, velocity, acceleration, etc.). The first portion of the time delay is designated as τ_1 and represents the time required to obtain measurements of the response. The second portion of the time delay is designated as τ_2 and represents the time required to apply the desired control force. At time t, the control computer determines the response of the structural system. Ideally, the measured response is $R(t)$. However the measured response actually occurred at time t_1 where the response is $R(t_1)$ and is being measured with a time delay due to, for example, signal conditioners, filters, differentiators, integrators, and computer computations. Also, at time t, the control computer determines the appropriate control signal to be sent to the control system. Ideally, the control is applied at time t. However, the control system does not respond instantaneously and actually applies the control force at time t_2 where the response is $R(t_2)$. Clearly, if time delays are not considered, control forces will be applied at time t_2 based on the response at time t_1.

The approach used herein to account for time delays is as follows: at time t, the controller receives information on the response measured at time t_1 and uses this information to predict the response at time t_2. The predicted response is based on experimentally measured values of time delays τ_1 and τ_2. Further, the predicted response is used to determine the appropriate control force to be applied at time t_2. Note that time delay compensation was employed only for tests in which the optimal control algorithm was utilized. Tests were performed without time delay compensation using both the optimal control algorithm and the sliding mode control algorithm.

5.1. Harmonic time delay compensation

The harmonic time delay compensation method is a simplified method which was developed by the authors and is based on the assumption that the structure responds as an undamped system in free vibration during the time interval between measuring the response and applying the control force. Clearly, this assumption is incorrect since the ground motion as well as the semi-active damper control forces act on the system during this time interval. However, if time delays are relatively small, the assumption of harmonic motion may be acceptable. Consider the relative displacement response vector of a Multi-Degree-of-Freedom (MDOF) structure which may be written in terms of modal coordinates as

$$\{u\} = [\Phi]\{y\} \tag{7}$$

where $\{y\}$ is the modal coordinate vector and $[\Phi]$ is the mode shape matrix. Letting $t_1 = 0$ and $t_2 = \tau$ (i.e. starting time at t_1), the free vibration response of the kth mode may be written as

$$y_k(\tau) = \frac{\dot{y}_k(0)}{\omega_k} \sin(\omega_k \tau) + y_k(0) \cos(\omega_k \tau) \tag{8}$$

where ω_k is the natural frequency of the kth mode. Note that τ is equal to the sum of time delays τ_1 and τ_2. The relative displacement vector is obtained as the sum of the modal contributions from each mode k:

$$\{u\} = \sum_{k=1}^{N} \{\phi_k\} y_k \tag{9}$$

where N is the number of modes and $\{\phi_k\}$ is the mode shape corresponding to the kth mode. At time $t = 0$, the value of the modal coordinate vector and its derivative can be obtained from equation (7). Combining the resulting expressions with equations (8) and (9), we obtain the predicted relative displacement of the jth degree of freedom in the following simple form:

$$u_j(\tau) = \sum_{i=1}^{N} [(a_i)_j u_i(0) + (b_i)_j \dot{u}_i(0)] \tag{10}$$

where $u_i(0)$ and $\dot{u}_i(0)$ are the relative displacement and relative velocity, respectively, of the ith degree of freedom at time $t = 0$ and $(a_i)_j$ and $(b_i)_j$ are constants corresponding to the jth degree of freedom and are determined from the modal frequencies, mode shapes, and measured time delays. Expressions similar to equation (10) can be developed to predict the relative velocity and relative acceleration corresponding to the jth degree of freedom.

5.2. *Experimentally measured time delays*

The response measurement time delay, τ_1, and the control force time delay, τ_2, were determined from experimental measurements of various time delays. Time delay τ_1 is considered to be the result of the following: signal conditioning, filtering, differentiating, and control computer computations. Time delay τ_2 is considered to be the result of delays in operation of the semi-active dampers.

The time delays associated with response measurement (signal conditioning (0·0 ms), low-pass filtering (21·0 ms), analog differentiation (3·9 ms)) and control computer computations (1·9–6·3 ms) are obtained by passing a white noise signal through each component of the system and obtaining the transfer function between the input and output signal. For white noise input, the transfer function between the input and output signal at frequency ω is given by

$$T(\omega) = \exp(\mathrm{i}\omega\tau_\mathrm{d}) \tag{11}$$

where τ_d is the time delay and i is the imaginary unit. The phase angle is given by

$$\theta(\omega) = \tan^{-1}\left(\frac{\Im[T(\omega)]}{\Re[T(\omega)]}\right) = \omega\tau_\mathrm{d} \tag{12}$$

where $\Im[\bullet]$ and $\Re[\bullet]$ indicate the imaginary and real parts of the contained complex quantity. Therefore, in components which exhibit a pure time delay, the amplitude of the transfer function is unity (equation (11)) and the phase angle is a linear function of frequency (equation (12)). The time delay is obtained from equation (12) using experimentally measured values of the phase angle.

The time delay associated with the development of the semi-active damper control force was determined by measuring the system response to a saturated command signal (i.e. a command signal which completely opens the value or completely closes the valve; thus modifying the damping coefficient from its maximum to minimum value and vice versa). The average time delay associated with modification of the control force was 20·3 ms.

6. SEISMIC SIMULATION TEST RESULTS

Selected seismic simulation test results are presented in this section. A more detailed presentation of results may be found in Reference 15. The benefits of using a semi-active control system can be assessed in many ways. In this study, a comparison of certain key response parameters are made for the structure with no dampers (bare frame), with two passive dampers (semi-active damper with fixed valve configuration), and with two semi-active dampers. The effect of the low and high damping passive control systems on the structure subjected to the El Centro ground motion is shown in Figure 6. The percentage figure shown in Figure 6 indicates the scale factor for the ground acceleration record (i.e. the ground acceleration for Figure 6

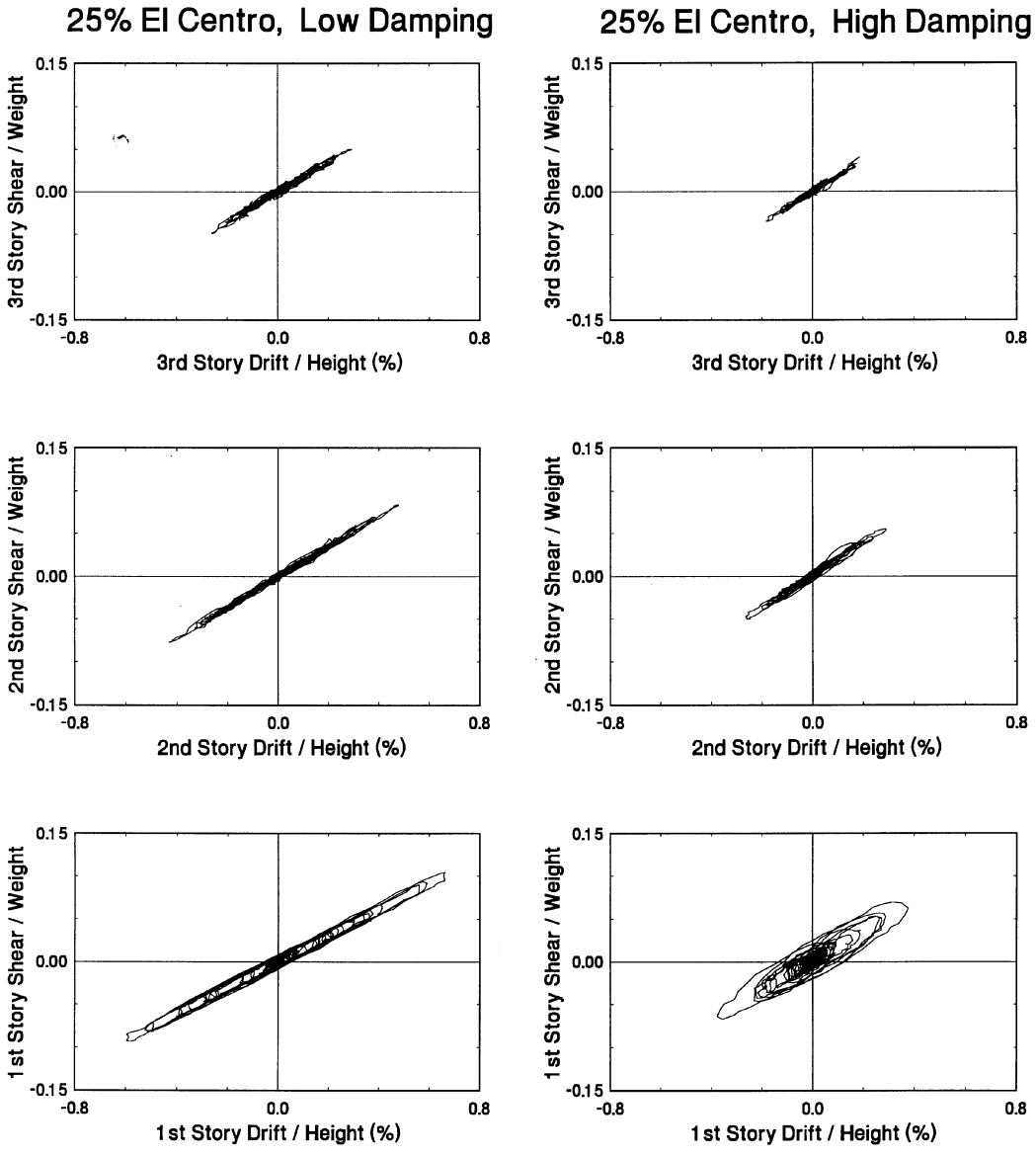

Figure 6. Seismic response of three-storey structure with passive damping

was scaled in magnitude by a factor of 25 per cent). Recall that the damping ratio in the fundamental mode of the three-storey structure with dampers set to low and set to high damping was about 4 and 14 per cent, respectively (see Table I). Note that friction is clearly present in the low damping test. This friction occurs between the piston rod and piston rod seal. In the high damping test, the primary source of energy dissipation appears to be through viscous fluid damping. A comparison between the low and high damping response of Figure 6 reveals that the first storey shear and first storey drift are reduced by factors of 1·5 and 1·8, respectively. Similar reductions are obtained in the second and third stories. The large increase in damping was clearly beneficial to the structure for this particular input. For the semi-active control algorithms employed in this study, the response reduction achieved by the semi-active control system was, in general, comparable to that afforded by the high damping passive control system.

Figure 7 presents peak response profiles of the three-storey structure subjected to seismic excitation and controlled by the semi-active dampers. Part (a) of Figure 7 compares response profiles of the Bare Frame (BF) structure, the structure with a Low Damping (LD) passive control system, and the structure with a High Damping (HD) passive control system. Part (b) compares response profiles of the bare frame structure with the structure controlled according to the Optimal Control Algorithm (OPT) with harmonic time delay compensation and the Sliding Mode Control algorithm (SMC). Recall that time-delay compensation was not utilized in tests which employed the sliding mode control algorithm. It is interesting to note, however, that the use of time-delay compensation in the optimal control tests typically produced minor improvements in the response (see Reference 15). Part (c) compares response profiles of the structure with a high damping passive control system to the structure controlled according to the same two semi-active control algorithms which are presented in part (b). The experimental results of Figure 7 were typical of the tests performed on the

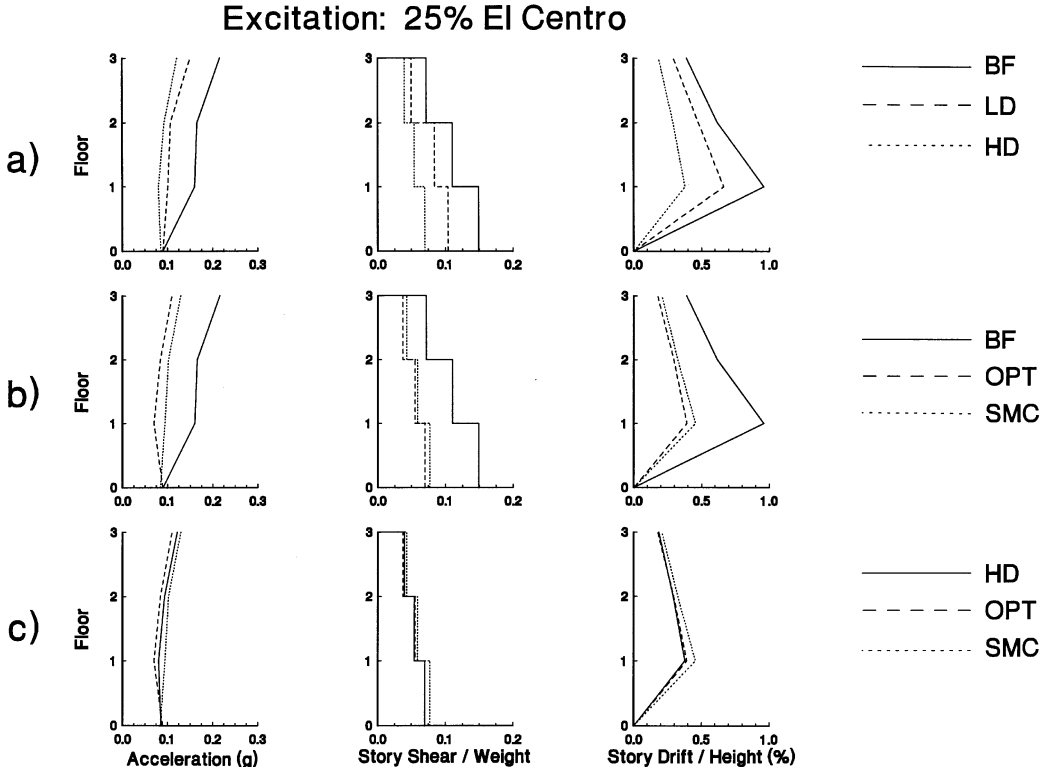

Figure 7. Peak response profiles of three-storey structure subjected to seismic motion

three-storey structure subjected to earthquake input (recall that a more detailed presentation of the experimental results is given in Reference 15) and thus one may conclude that:

(1) The response of the bare frame structure is significantly reduced with the addition of the passive high damping control system (see part (a) of Figure 7).
(2) The response of the bare frame structure is significantly reduced with the addition of the semi-active control systems (see part (b) of Figure 7).
(3) The response of the structure with the passive high damping control system is typically less than or nearly the same as the response obtained with the semi-active control systems (see part (b) of Figure 7).

Evidently, the use of a semi-active control system offered no significant advantage over the use of a high damping passive control system. Similar conclusions were made by Polak *et al.*[26] in a numerical study on a three-storey structure with a semi-active damping system. However, the authors of that study note that, under certain special conditions (e.g. at soil sites in which resonances can be expected but the resonant frequency is difficult to establish), a semi-active damping system may be warranted.

The future implementation of semi-active control systems will require that the systems be robust with respect to measurement errors. This issue was explored in a test on the three-storey structure subjected to the Hachinohe ground motion (see Figure 8). In Figure 8(a), a comparison is made between the passive high damping control system response and the semi-active control system response using the optimal control algorithm without time-delay compensation. As discussed previously, the response of the three-storey structure with a semi-active control system is nearly the same as the response with a passive high damping

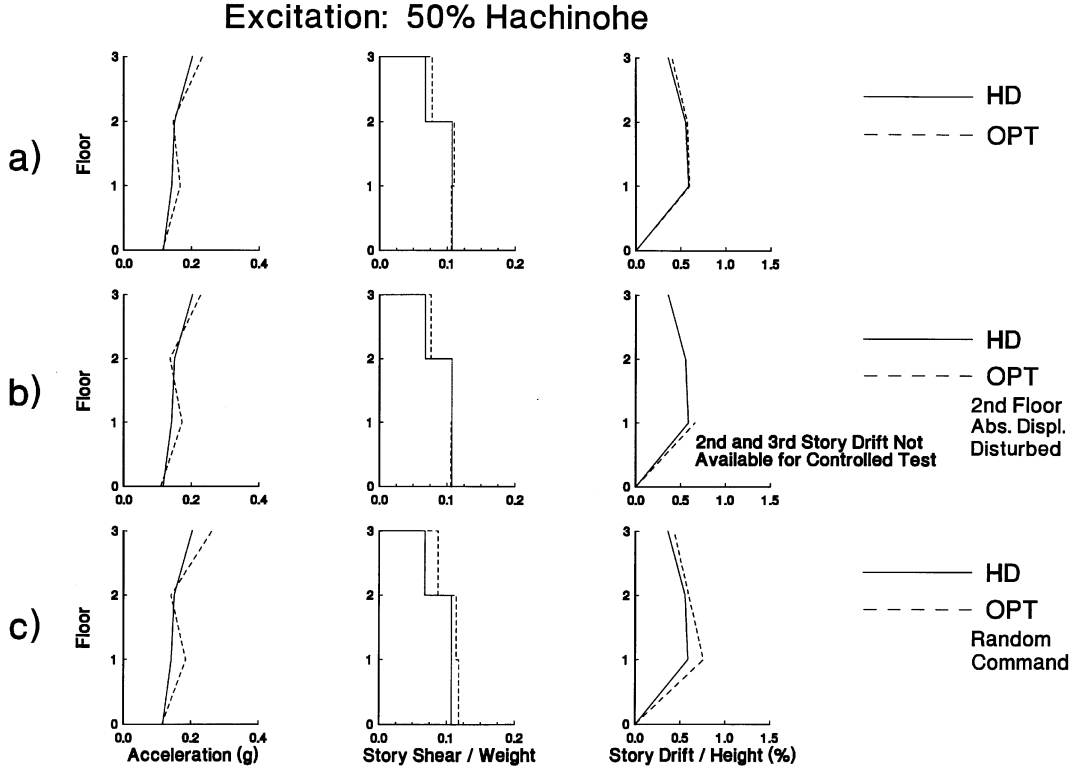

Figure 8. Verification of robust behaviour of three-storey structure with semi-active control system

control system. In Figure 8(b), the same comparison is made as in Figure 8(a) except with the second floor absolute displacement signal disturbed during the semi-active control test (the disturbance was caused by randomly moving the external magnet assembly of the linear displacement transducer during the shaking table test). Recall that analogue differentiators are used to obtain the total velocity at each floor level. Therefore, both the second floor displacement and velocity were affected by the disturbance. It is apparent from Figure 8(b) that the measurement errors caused by the disturbance did not adversely affect the response of the structure (maximum peak acceleration increase of about 4 per cent, no increase in peak shear force, and a peak drift increase at the first storey of about 11 per cent). A different disturbance was produced by randomly adjusting the command signal to the semi-active damper valves during the semi-active control test (see Figure 8(c)). A valve command signal was generated by the control computer but the power supply to the valve control circuits was turned on and off randomly to allow or not allow, respectively, the valve command signal to be sent to the valve. The effect of the random command was to increase peak accelerations and peak shear forces by about 12 per cent and peak drifts by about 28 per cent.

7. ANALYTICAL PREDICTIONS OF SEISMIC SIMULATION TEST RESULTS

Analytical predictions of the shaking table test results were obtained using two different methods. One method assumes that, at each time step in the analysis, the response is measured instantaneously, a command signal is determined instantaneously, and the semi-active dampers respond instantaneously. This type of control is ideal but cannot be realized in the laboratory. The analytical predictions associated with this method are designated as 'instantaneous' control predictions. A second method for analytical predictions was developed to take into the account the inherent time delays associated with dynamic control systems. This method assumes that, at each time step in the analysis, the response is measured with a time delay, the command signal is generated based on the delayed response, and the semi-active dampers respond with both a static and dynamic time delay (the static time delay corresponds to a period of time after which the command signal has been sent to the valve but during which the valve spool does not move). Further, it is assumed that the semi-active control valves are not capable of responding to a command signal if they are currently responding to a previous command signal. Analytical predictions were obtained by numerically solving the set of differential equations describing the system.[27] The predictions which include the effect of time delays generally produced results that are in closer agreement with the experimentally measured results than the predictions obtained under the assumption of instantaneous control.

The equation of motion for the three-storey structure with semi-active dampers is given as follows where it is assumed that the structure behaves as a shear-type building

$$[M]\{\ddot{u}\} + [C_u]\{\dot{u}\} + [K]\{u\} + \{P_d\} = -[M]\{1\}\ddot{u}_g \tag{13}$$

where $[M]$ is the mass matrix, $[C_u]$ is the damping matrix of the bare frame structure, $[K]$ is the stiffness matrix, $\{P_d\}$ is the control force vector, $\{1\}$ is a vector of units, $\ddot{u}_g$ is the ground acceleration, and $\{\ddot{u}\}$, $\{\dot{u}\}$ and $\{u\}$ are the relative acceleration, velocity, and displacement vectors, respectively. For the case of two semi-active dampers in the first storey, the damper force vector is given by

$$\{P_d\} = \begin{Bmatrix} 0 \\ 0 \\ 2P_1 \end{Bmatrix} \tag{14}$$

where P_1 is the horizontal component of damper force in a single damper in the first storey. As mentioned previously, the semi-active dampers behave essentially as linear viscous dampers with an adjustable damping coefficient. However, as the frequency of motion is increased, the dampers begin to develop stiffness. This can be accounted for by utilizing a Maxwell fluid model for describing the damper behavior (see Reference 15)

$$P_1 + \lambda \dot{P}_1 = C_{SA} \cos^2 \theta \dot{u}_1 \tag{15}$$

where λ is the relaxation constant. Equations (13)–(15) can be written as a set of first-order differential equations

$$\{\dot{Z}\} = [A]\{Z\} + [H]\{f\} \tag{16}$$

where

$$[Z] = \begin{Bmatrix} \{\dot{u}\} \\ \{u\} \\ \{P_d\} \end{Bmatrix} \tag{17}$$

$$[A] = \begin{bmatrix} -[M]^{-1}[C_u] & -[M]^{-1}[K] & -[M]^{-1} \\ [I] & [0] & [0] \\ \lambda^{-1}[C] & [0] & -\lambda^{-1}[I] \end{bmatrix} \tag{18}$$

$$[H] = \begin{bmatrix} [I] \\ [0] \\ [0] \end{bmatrix} \tag{19}$$

$$\{f\} = \{1\}\,\ddot{u}_g \tag{20}$$

and

$$[C] = \begin{bmatrix} 0 & 0 & 0 \\ 0 & 0 & 0 \\ 0 & 0 & 2\,C_{SA}\cos^2\theta \end{bmatrix} \tag{21}$$

Note that $[I]$ and $[0]$ represent the identity and null matrix, respectively. Analytical predictions for the three-storey structure were obtained by numerically solving the set of differential equations described by equation (16). The stiffness and damping matrix of the structure, $[K]$ and $[C_u]$ in equation (13), were obtained from experimentally determined frequencies, damping ratios, and mode shapes. The numerical solution provides the response history of the quantities in vector $\{Z\}$ (i.e. the relative displacement vector, the relative velocity vector, and the vector of horizontal component of force from the semi-active dampers). The total acceleration vector is computed from equation (16) and is used in calculation of the story shear forces.

Experimental results are compared with analytical predictions in Figure 9 for the three-storey structure with semi-active dampers subjected to the El Centro ground motion and controlled according to the optimal control algorithm without time-delay compensation. The two different analytical methods previously described were used to obtain the analytical predictions. In the first method, instantaneous control was assumed. Although instantaneous control cannot be realized in the laboratory, it does represent the ideal response for the given semi-active control algorithm. In the second method, experimentally measured time delays were utilized. The two methods produce very similar results and compare reasonably well with the experimental results. Of course, the experimentally measured delays for the semi-active dampers were obtained in saturated command signal tests in which a single command signal was applied to the control valve (see Section 5.2 and Reference 15). During the shaking table tests, however, the command signal to the control valves was updated at time intervals of approximately 2–6 ms. Lack of knowledge regarding the

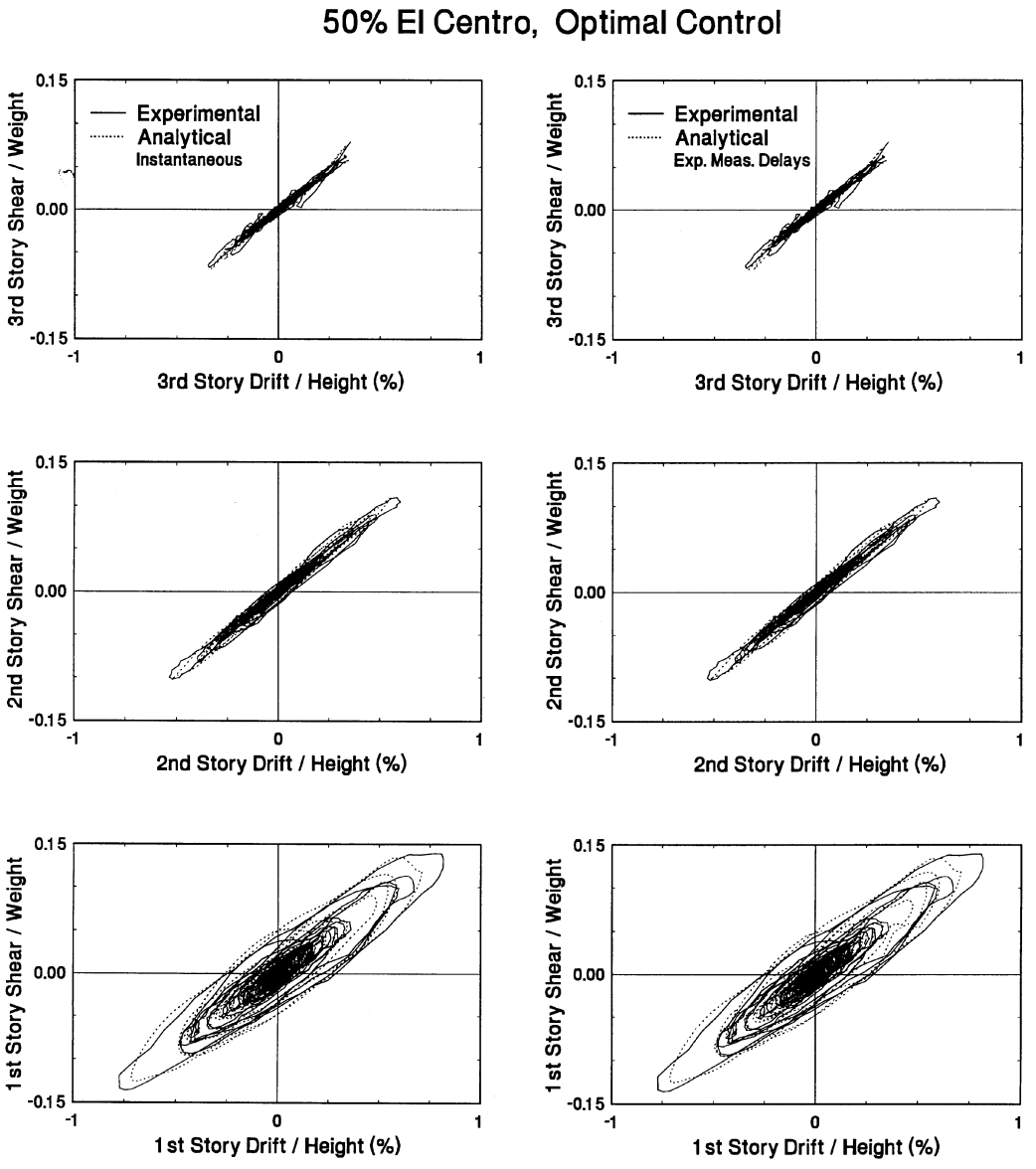

Figure 9. Comparison of experimental and analytical response of three-storey structure with a semi-active control system

behaviour of the control valves under such high frequency command signals inhibited the analytical prediction of experimental results. The analytical predictions may be further improved by developing an improved analytical model for the semi-active damper that explicitly accounts for the dynamics of the servovalve.

8. COMPARISON WITH AN ACTIVE CONTROL SYSTEM

A comparison can be made between the results from the semi-active control tests described in this paper and previous results obtained from active control tests on the same structure in which an active tendon control

Table II. Comparison of properties of three-storey structure used in active and semi-active control tests

		System parameters					
		Frequency (Hz)			Damping ratio (%)		
	Control system	Mode 1	Mode 2	Mode 3	Mode 1	Mode 2	Mode 3
Active control tests	Bare frame	2·20	6·80	11·50	1·60	0·39	0·36
	Active tendon system	2·28	6·94	11·56	12·77	12·27	5·45
Semi-active control tests	Bare frame	1·80	5·80	11·40	1·74	0·76	0·34
	High passive damping	1·85	6·04	11·48	14·41	18·79	4·83

system was utilized in combination with a linear optimal control algorithm similar to that described in Section 4.1.[21,22,28] The properties of the three-storey structure described in this paper are compared in Table II with the properties of the same structure when it was tested using an active control system. Note that the dynamic characteristics of the bare frame structure exhibited some small changes during the interim between the two testing programs. A comparison of seismic response profiles for the two systems is presented in Figure 10 for the El Centro ground motion. The percentage figures shown in Figure 10 indicate the peak response reduction in comparison with the bare frame structure response. Figure 10(a) shows that the active tendon system significantly reduces the peak response as compared with the bare frame structure. Further, Figure 10(b) shows that the peak response reduction obtained with the high damping passive control system surpasses the reduction obtained with the active tendon system. Finally, Figure 10(c) shows results for the semi-active control system in which the optimal control algorithm without time delay compensation was utilized. Recalling Section 4.1, the optimal control algorithm used in the semi-active control test of Figure 10(c) is identical to that used in the active tendon control test of Figure 10(a) except that, for the semi-active control test, the damping coefficient is bounded according to equation (1). The results of Figures 10(a) and 10(c) indicate that the semi-active control system was capable of achieving larger reductions in peak response in comparison to the active control system in which the same control algorithm was utilized. This was simply the result of larger effective damping in the semi-active control system. Interestingly, the semi-active control system produced peak response reductions which are nearly identical to those obtained with the high damping passive control system (compare Figures 10(b) and 10(c)). Apparently, the high damping passive control system was more efficient than the active or semi-active control systems for this particular structure, excitation, and control algorithm.

9. CONCLUSIONS

A small scale model of a moment-resisting frame outfitted with a semi-active control system was tested with seismic ground motion supplied by a large shaking table. The semi-active control system was in the form of fluid dampers which were capable of developing a wide range of damping levels between an upper and lower bound. The results from shaking table tests demonstrated the following:

(1) The response of the structure with no dampers (bare frame) was dramatically improved with the addition of the semi-active damper control system.
(2) The response reductions achieved with the semi-active control system were comparable to those obtained with a high damping passive control system (as measured by peak response quantities). It is expected that further response reductions beyond those afforded by a passive control system can be

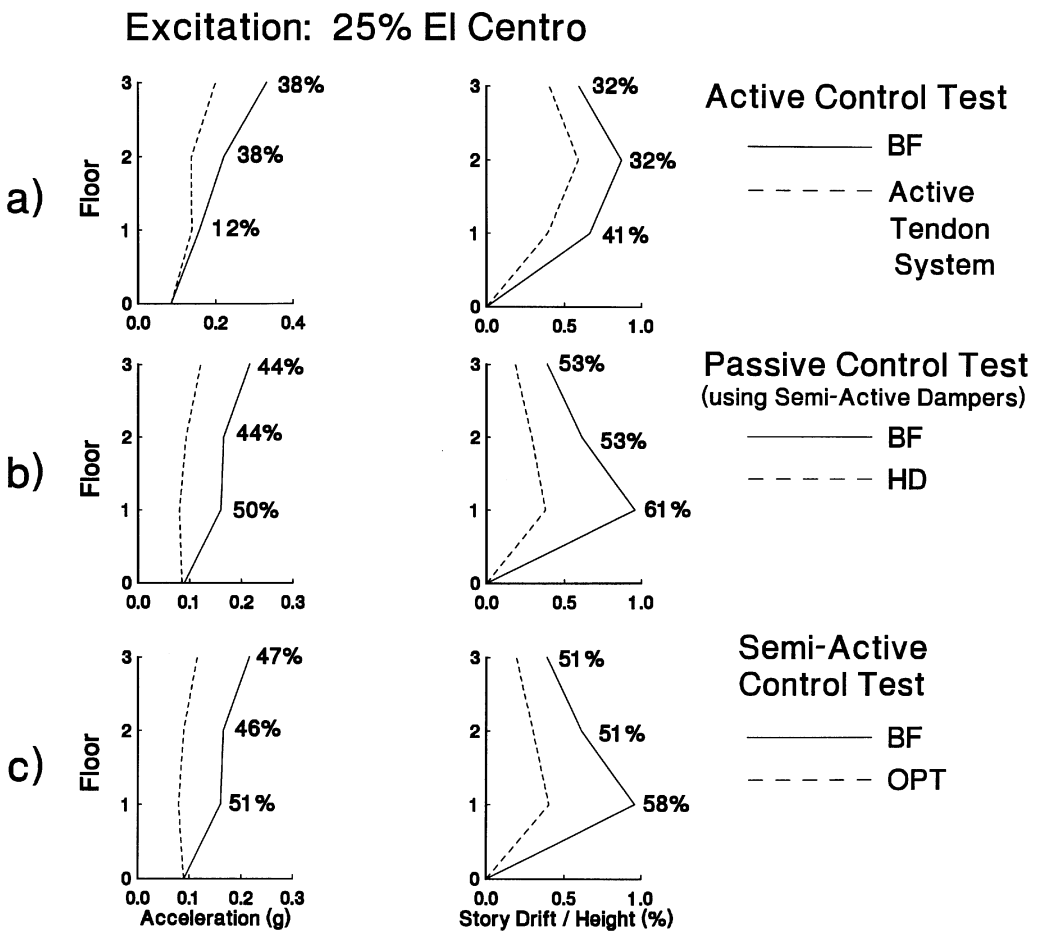

Figure 10. Comparison of response of three-storey structure controlled by (a) an active control system, (b) a passive control system, and (c) a semi-active control system

achieved through improved control algorithms (e.g. by incorporating the constraint on the damping coefficient), improved semi-active damper hardware, and improved methods of accounting for time delays either directly through improved modelling of the dynamics of the control system or indirectly through improved time-delay compensation methods. In addition, one may easily reduce time delays associated with response measurement by utilizing digital filters rather than analogue filters. Furthermore, this study was limited to a specific type of structural system which was subjected to a limited range of ground motion characteristics. There may be other conditions in which the use of semi-active dampers may prove advantageous.

(3) The use of time delay compensation typically produced minor improvements in the response and, in some cases (not reported herein), degraded the response. The implementation of time delay compensation in a feedback control system requires a good estimate of the time delays associated with each component of the control system. The time delays associated with response measurements had well-defined values. In contrast, the semi-active damper time delays were not as well defined and average values from command signal saturation tests were used in the shaking table tests which employed time delay compensation. Moreover, the time delay compensation method utilized in this study was based on certain simplifying assumptions and thus was approximate in nature.

(4) The semi-active control system was robust with respect to measurement disturbances and command signal disturbances in the sense that the structural system did not become unstable as a result of the disturbances. Stability is generally not a concern in control systems which can only extract energy from the structural system. In contrast, the servohydraulic actuators used within active control systems are capable of supplying energy to the structural system and thus the issue of stability must be addressed.
(5) The semi-active damper control system produced larger response reductions in the three-storey structure compared to those obtained with an active tendon control system wherein both control systems were designed according to optimal control theory. The difference in response of the semi-active and active control systems was simply the result of larger effective damping in the semi-active control system.

Finally, the importance of comparing the response of structures with semi-active and active control systems to structures with properly designed passive control systems must be stressed. Only then can the benefits of these technologies be assessed and reported in a form which is useful to the profession.

ACKNOWLEDGEMENTS

Financial support for this work was provided by the National Center for Earthquake Engineering Research (Project Numbers 93-5120 and 94-5103A), Taylor Devices, Inc., N. Tonawanda, NY and Moog Inc., E. Aurora, NY. Furthermore, Taylor Devices, Inc. and Moog Inc. donated equipment which was used during the experimental portion of the research project. The assistance and cooperation of Mr. Douglas P. Taylor (President, Taylor Devices, Inc.) and Mr. Kenneth D. Garnjost (Vice President for Engineering, Moog Inc.) is gratefully acknowledged.

REFERENCES

1. D. Hrovat, P. Barak and M. Rabins, 'Semi-active versus passive or active tuned mass dampers for structural control', *J. eng. mech., ASCE*, **109**(3), 691–705 (1983).
2. T. Mizuno, T. Kobori, J. Hirai, M. Yoshinori and N. Niwa, 'Development of adjustable hydraulic damper for seismic response control of large structures', in *PVP-Vol. 229, DOE Facilities Programs, Systems Interaction, and Active/Inactive Damping*, ASME, New Orleans, LA, June, 1992, pp. 163–170.
3. S. Rakheja and A. K. Ahmed, 'Simulation of non-linear variable dampers using energy similarity', *Eng. comput.* **8**, 333–344 (1991).
4. K. Hasewaga and J. M. Kelly, 'Application of a mass damping system to bridge structures', *Report No. UBC/EERC-92/12*, Earthquake Engineering Research Center, University of California, Berkeley, 1992.
5. M. Shinozuka and R. Ghanem, 'Use of variable dampers for earthquake protection of bridges', in *Proc. 2nd U.S.–Japan workshop on earthquake protective systems for bridges*, Public Works Research Institute, Tsukuba Science City, Japan, December, 1992, pp. 507–516.
6. Z. Akbay and H. M. Aktan, 'Actively regulated friction slip braces', in *Proc. Sixth Canadian conf. on earthquake eng.*, Toronto, Canada, June, 1991, pp. 367–374.
7. W. N. Patten, R. L. Sack, W. Yen, C. Mo and H. C. Wu, 'Seismic motion control using semi-active hydraulic force actuators', in *Proc. seminar on seismic isolation, passive energy dissipation, and active control, Report No. ATC-17-1*, Applied Technology Council, San Francisco, CA, March, 1993, pp. 727–736.
8. M. Q. Feng and M. Shinozuka, 'Experimental and analytical study of a hybrid isolation system using friction controllable sliding bearings', *Report No. NCEER 92-0009*, National Center for Earthquake Engineering Research, Buffalo, NY, 1992.
9. T. Kobori, M. Takahashi, T. Nasu and N. Niwa, 'Seismic response controlled structure with active variable stiffness', *Earthquake Engng. Struct. Dyn.*, **22**, 925–941 (1993).
10. H. P. Gavin, Y. D. Hose and R. D. Hanson, 'Design and control of electrorheological dampers', in *Proc. 1st world conf. on structural control*, Los Angeles, CA, August, WP3-83–WP3-92, 1994.
11. N. Makris, D. Hill, S. Burton and M. Jordan, 'Electrorheological fluid damper for seismic protection of structures', in *Proc. smart structures and materials conf.*, San Diego, CA, February, 1995, pp. 184–194.
12. K. Kawashima, S. Unjoh, H. Iida and H. Mukai, 'Effectiveness of the variable damper for reducing seismic response of highway bridges', in *Proc. 2nd U.S–Japan workshop on earthquake protective systems for bridges*, PWRI, Tsukuba Science City, Japan, December, 1992, pp. 479–493.
13. W. N. Patten, R. L. Sack and Q. He, 'Controlled semiactive hydraulic vibration absorber for bridges', *J. struct. eng.* **122**(2), 187–192 (1996).

14. B. F. Spencer, S. J. Dyke, M. K. Sain and J. D. Carlson, 'Dynamic model of a magnetorheological damper', in *Proc. 12th conf. on analysis and computation held in conjunction with structures congress XIV*, ASCE, Chicago, IL, April, pp. 361–370.
15. M. D. Symans and M. C. Constantinou, 'Development and experimental study of semi-active fluid damping devices for seismic protection of structures', *Report No. NCEER 95-0011*, National Center for Earthquake Engineering Research, Buffalo, NY, 1995.
16. M. C. Constantinou and M. D. Symans, 'Experimental study of seismic response of buildings with supplemental fluid dampers', *Struct. Design Tall Build.*, **2**, 93–132 (1993).
17. M. C. Constantinou and M. D. Symans, 'Seismic response of structures with supplemental fluid viscous dampers', *NCEER Report No. 92-0032*, National Center for Earthquake Engineering Research, Buffalo, NY, 1992.
18. P. Tsopelas, S. Okamoto, M. C. Constantinou, D. Ozaki and S. Fujii, 'NCEER-Taisei Corporation research program on sliding seismic isolation systems for bridges: experimental and analytical study of systems consisting of sliding bearings, rubber restoring force devices and fluid dampers', *NCEER Report No. 94-0002*, National Center for Earthquake Engineering Research, Buffalo, NY, 1994.
19. T. T. Soong, A. M. Reinhorn and J. N. Yang, 'A standardized model for structural control experiments and some experimental results', in *Proc. 2nd int. symp. on structural control*, 1985, Waterloo, Canada, 1987, pp. 669–693.
20. T. Fujita, M. Shimazaki, Y. Hayamizu, S. Aizawa, M. Higashino and H. Nobuyoshi, 'Semiactive seismic isolation system using controllable friction damper', *Bull. earthquake resistant struct. res. center*, No. 27, 21–31, March, 1994.
21. T. T. Soong and M. C. Constantinou, *Passive and Active Structural Vibration Control in Civil Engineering*, Springer, Wien, 1994.
22. T. T. Soong, *Active Structural Control: Theory and Practice*, Longman, New York, 1990.
23. R. Ghanem and M. Bujakov, 'Adaptive control of non-linear dynamical systems with uncertainties', in *Proc. 1st world conf. on structural control*, Los Angeles, CA, August, 1994, TA4-23–TA4-32.
24. S. McGreevy, T. T. Soong and A. M. Reinhorn, 'An experimental study of time delay compensation in active structural control', in *Proc. 6th int. modal analysis conf.*, Vol. 1, Orlando, FL, 733–739, 1988.
25. A. M. Reinhorn, T. T. Soong, R. C. Lin, M. A. Riley, Y. P. Wang, S. Aizawa and M. Higashino, 'Active bracing system: a full scale implementation of active control', *Report No. NCEER 92-0020*, National Center for Earthquake Engineering Research, Buffalo, NY, 1992.
26. E. Polak, G. Meeker, K. Yamada and N. Kurata, 'Evaluation of an active variable-damping structure', *Earthquake Engng. Struct. Dyn.*, **23**, 1259–1274 (1994).
27. IMSL, International Mathematical and Statistical Library, Subroutine IVPAG, Houston, TX, 1987.
28. L. L. Chung, R. C. Lin, T. T. Soong and A. M. Reinhorn, 'Experimental study of active control for MDOF seismic structures', *J. eng. mech., ASCE*, **115**(8), 1609–1627 (1989).

